Prediction of phase formation sequence and phase stability in binary metal-aluminum thin-film systems using the effective heat of formation rule

R. Pretorius,[a] A. M. Vredenberg, and F. W. Saris
FOM-Institute for Atomic and Molecular Physics, Kruislaan 407, 1098 SJ Amsterdam, The Netherlands

R. de Reus
Physics Department, Riso National Laboratory, DK-4000 Roskilde, Denmark

The effective heat of formation ($\Delta H'$) concept allows heats of formation to be calculated as a function of concentration. In this work the effective heat of formation rule is used to predict first phase formation in metal-aluminum thin-film systems and to predict subsequent phase sequence for thin metal films on thick aluminum or thin aluminum on thick metal substrates. The effective concentration at the growth interface is taken to be that of the lowest temperature eutectic (liquidus) for the binary system. Although the effective heat of formation rule may predict that formation of a certain phase would lead to the largest free energy change, this phase does not necessarily form at the moving reaction interface if it has difficulty to nucleate. By excluding phases with a large number of atoms per unit cell and which thus have difficulty to nucleate, the effective heat of formation rule successfully predicts first phase aluminide formation for all 15 metal-aluminum binary systems for which experimental data could be found. It is also shown how the effective heat of formation rule can be used to predict formation and decomposition of aluminide phases in contact with each other or in contact with their component metals.

I. INTRODUCTION

There has been much interest in formulating rules for predicting first phase formation and subsequent phase sequence in binary metal-silicon[1-5] and metal-metal[6,7] thin-film systems. One of the first rules[1] was that of Walser and Bené which stated that:

"The first compound nucleated in planar binary reaction couples is the most stable congruently melting compound adjacent to the lowest-temperature eutectic on the bulk equilibrium phase diagram."

This rule was relatively successful in predicting first phase formation in metal-silicon systems and was extended by Tsaur et al.[2] to subsequent phase formation sequence in metal-silicon systems using the smallest temperature difference between the liquidus curve and the peritectic (or peritectiod) point as a measure of stability when the compounds between the first phase and the remaining element are all noncongruently melting compounds. Bené subsequently extended the Walser-Bené rule to metal-metal systems[6] by relaxing the requirement that the first phase that forms needs to be congruent. Later Ronay[3] proposed a rule for first phase nucleation taking into account the central eutectic, diffusing species, and interfacial free energy. None of the above-mentioned rules did, however, make direct use of thermodynamic data and it was only after Pretorius[4,5,7] proposed the effective heat of formation concept that thermodynamic data could be used directly to predict first phase formation and the subsequent phase sequence. The effective heat of formation rule enables the calculation of heats of formation as a function of concentration and has been successful in predicting silicide phase formation sequence[4,5] and to explain how the presence of impurities such as oxygen or small amounts of gold can alter phase formation sequence during nickel and cobalt silicide formation, respectively.[5] It has also been useful in explaining why CoSi formation is dominant at low temperatures while the formation of Co_2Si becomes significant at higher temperatures during ion-beam mixing in the Co-Si system.[8] Recently the effective heat of formation concept was used to predict phase formation in Al-Ni systems.[7] In this work we test the effective heat of formation rule by comparing its predictions against experimental data for metal-Al systems in general.

II. THE EFFECTIVE HEAT OF FORMATION RULE

The driving force for a process to take place is given by the change in the Gibbs free energy:

$$\Delta G^\circ = \Delta H^\circ - T \Delta S^\circ, \tag{1}$$

where ΔH° is the change in enthalpy during the reaction at temperature T and ΔS° the change in entropy. The change in enthalpy (or heat of formation) ΔH° is, however, a good measure of the change in free energy ΔG° because the change in entropy ΔS° is usually only about ± 0.001 kJ/deg per mole of atoms during solid state formation of ordered compounds.[9] The term $T \Delta S^\circ$ at a typical reaction temperature of 300 °C is thus usually negligibly small when compared to heats of formation ΔH° for most solid state reactions (see Tables I and II for aluminide ΔH° values). It should therefore be possible to use heats of formation to predict phase formation when activation or nucleation barriers do not exist, as a system would always want to go to its lowest possible free energy state. During solid-state in-

[a] On leave from the Ion-solid Interaction Division, Van de Graaff Group, National Accelerator Centre, P.O. Box 72, Faure 7131, South Africa.

TABLE I. Effective heats of formation ($\Delta H'$) for zirconium-aluminide compounds, calculated at two different concentrations of the reacting elements.[a]

| Phase | Effective Concentrations | | | $Zr_{0.020}Al_{0.980}$ | | $Zr_{0.500}Al_{0.500}$ | |
	Compound concentration	ΔH° kJ(mol at.)$^{-1}$	Limiting element	$\Delta H'$ kJ(mol. at.)$^{-1}$	Limiting element	$\Delta H'$ kJ(mol at.%)$^{-1}$
Zr_5Al_3	$Zr_{0.625}Al_{0.375}$	-39	Zr	-1.25	Zr	-31.2
Zr_3Al_2	$Zr_{0.600}Al_{0.400}$	-41	Zr	-1.37	Zr	-34.2
Zr_4Al_3	$Zr_{0.571}Al_{0.429}$	-43	Zr	-1.51	Zr	-37.7
ZrAl	$Zr_{0.500}Al_{0.500}$	-45	Zr	-1.80	$\cdots$	-45.0
Zr_2Al_3	$Zr_{0.400}Al_{0.600}$	-47	Zr	-2.35	Al	-39.2
$ZrAl_2$	$Zr_{0.333}Al_{0.667}$	-46	Zr	-2.76	Al	-34.5
$ZrAl_3$	$Zr_{0.250}Al_{0.750}$	-41	Zr	-3.28	Al	-27.3

[a]Heats of formation (ΔH°) from Refs. 25 and 31.

teraction, phase formation at an interface is a nonequilibrium process. In the case of silicide formation, for instance, it is always found that only one compound phase forms at a particular interface,[10] which is unlike equilibrium systems where simultaneous formation of a mixture of phases can lead to the lowest free energy state for the system.

Let us now, as an example, consider the solid state interaction between Zr and Al. According to the phase diagram of this binary system,[11] there are nine possible equilibrium compound phases that can form at the growth interface. In the effective heat of formation concept single phase formation and the available (effective) concentrations of Zr and Al at the growth interface is taken into account when considering the free energy change of the system during interaction.[4,5,7] If we, for example, consider the formation of the compound phase $ZrAl_2$ and assume that the effective concentration of Zr at the growth interface is 50 at. % and Al is 50 at. %, we have that:

Heat of formation (ΔH°) = -46 kJ(mol at.)$^{-1}$;
Compound to be formed = $Zr_{0.333}Al_{0.667}(ZrAl_2)$;
Effective concentrations = $Zr_{0.500}Al_{0.500}$;

therefore, the limiting element is Al.

It is clear that for the conditions as defined above, all the Al atoms will be used up at the interface during $ZrAl_2$ formation and the Zr atoms will be in excess. Aluminum is therefore the limiting element. It should, however, again be emphasized that phase formation at a growth interface is a dynamic nonequilibrium process and the "excess" atoms should be looked upon as being available for formation of the next increment of the compound at the moving interface. It can thus be seen that the heat released is dictated by the effective concentration of the limiting element and the concentration of the limiting element in the compound to be formed. An effective heat of formation ($\Delta H'$) can therefore be defined[4,5,7] as:

$$\Delta H' = \Delta H^\circ \times \left(\frac{\text{effective conc. lim. element}}{\text{compound conc. lim. element}} \right). \quad (2)$$

For the above-mentioned case where the relative available concentrations at the growth interface is 50 at. % Zr and 50 at. % Al, the effective heat of formation for growth of $ZrAl_2$ is given by

$$\Delta H' = \Delta H^\circ (0.500/0.667) = -34.5 \text{ kJ(mol at.)}^{-1}. \quad (3)$$

With Eq. (2) the effective heat of formation of any compound can now be calculated as a function of the concentration of the reacting species. This is illustrated in Table I where the effective heats of formation ($\Delta H'$) have been calculated for the zirconium aluminide phases (except for Zr_2Al and Zr_3Al for which ΔH° values were not available) at two different concentrations. For a Zr concentration of 2 at. %, formation of $ZrAl_3$ is expected to take place as it has the most negative $\Delta H'$ of -3.28 kJ(mole of atoms)$^{-1}$, while ZrAl formation will lead to the lowest free energy state for the system if experimental conditions are such that the effective concentration of Zr is 50 at. %. Such calculations can be represented graphically and the effective heat of formation diagram for the Zr-Al system, together with its phase diagram, is given in Fig. 1. It can be seen that for each phase the most negative $\Delta H'$ and thus the release of the most energy from the system occurs when the Zr and Al concentrations match that of a particular compound, as $\Delta H' = \Delta H^\circ$ [see Eq. (2)]. Effective heats of formation diagrams are thus very easily constructed by plotting the heats of formation ΔH° (expressed in kJ per mole of atoms) of each compound in the binary system at its compositional concentration and completing the triangulation by connecting these points to the end points of the concentration axis.

III. PREDICTION OF PHASE FORMATION

A. First phase formation

To predict phase formation using the effective heat of formation concept, it is necessary to know what the effective concentrations are of the two reacting species at the growth interface. It should however be remembered that thin-film solid state interaction is a nonequilibrium process and the effective concentration at the growth interface is independent of the relative thicknesses of the interacting components. Many factors such as lowest eutectic, impurities, atomic mobility, diffusing species, etc., could affect the actual concentrations that are available for interaction at the growth interface. This is the reason why the term effective concentration is used in the effective heat of formation concept, which is similar to the effective concentration concept used in solution chemistry, where the effective concentration can differ greatly from the true
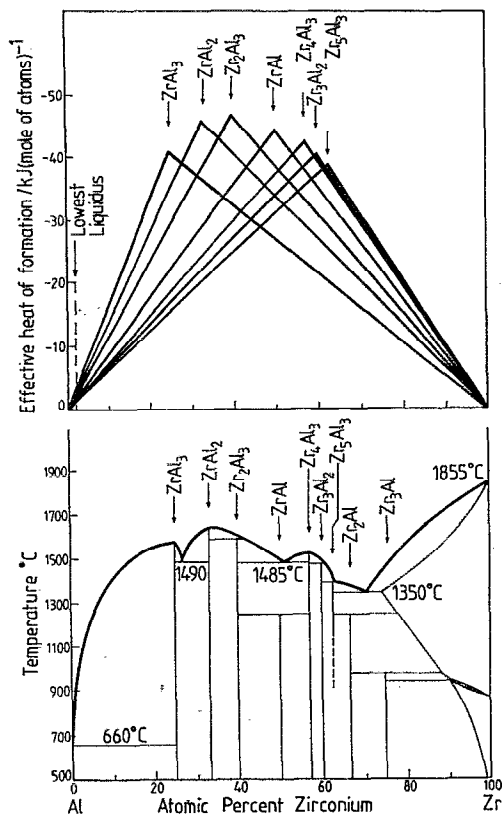
FIG. 1. The effective heat of formation ($\Delta H'$) diagram for compound phase formation (top) and the phase diagram (bottom) for the Zr-Al system. Each triangle of the effective heat of formation diagram represents the energy released during the formation of a particular zirconium-aluminide phase as a function of concentration. The most negative $\Delta H'$ values occur when the Zr and Al concentrations match that of a particular compound, as the ratio of effective concentration and compound concentration is unity [see Eq. (2)] and the effective heat of formation ($\Delta H'$) is then equal to the heat of formation (ΔH°) expressed as kJ (mol at.)$^{-1}$.

concentration, the two concentrations being linked by an activity coefficient. It is not possible to calculate what the actual effective concentrations of the reactants are at the growth interface during solid state interaction. Brown and Ashby have, however, shown that for a given structure and bond type, the activation energy for solid state diffusion is directly proportional to the melting point of the solid.[12] Assuming that the pre-exponential factor in the diffusion coefficient is approximately the same, the activation energy determines mobility. The greatest mobility of the atoms and the most effective mixing at a reaction interface upon heating is therefore expected to take place at the composition of the lowest eutectic (or liquidus) of the binary system. We therefore choose the effective concentrations of the interacting atoms to be that of the lowest temperature eutectic (liquidus). This is also the criterion used in the Walser-Bené phase formation rule.[1] From the Al-Zr phase diagram (see Fig. 1) it can be seen that the lowest temperature on the liquidus curve is 660 °C, which corresponds to the melting point of pure aluminum. The relative concentrations of the reacting species at the growth interface are

therefore expected to be very Al rich and in such a case (where there is not a lowest temperature eutectic) we arbitrarily choose an effective aluminum concentration of 98 at. %. This is indicated by the arrow labeled lowest liquidus in the effective heat of formation diagram (top, Fig. 1). The first column of $\Delta H'$ values in Table I has been calculated at this concentration (98 at. % Al, 2 at. % Zr) and it can be seen that formation of the most Al-rich phase $ZrAl_3$ gives the most negative effective heat of formation of -3.28 kJ (mol at.)$^{-1}$ This is also the phase that is found to form experimentally.[6,13,14] The rule for first phase formation thus states:[7]

"*The first-compound phase to form during metal-metal interaction is the phase with the most negative, effective heat of formation ($\Delta H'$) at the concentration of the lowest temperature eutectic (liquidus) of the binary system.*"

B. Phase formation sequence

To illustrate how the effective heat of formation rule can be used to predict phase formation sequence, let us again consider the Zr-Al system. For the case of a thin Al film on thick Zr (Al < Zr) a stage during interaction will be reached when all the Al will be consumed during first phase $ZrAl_3$ formation. At this stage the effective Al concentration at the Zr/$ZrAl_3$ interface is expected to decrease moving to the right of the effective heat of formation diagram (see Fig. 1) until an effective concentration of about 71 at. % Al and 29 at. % Zr is reached. At this concentration the effective heat of formation diagram shows that $ZrAl_2$ formation should lead to the most negative effective heat of formation. After transformation of all the $ZrAl_3$ to $ZrAl_2$ the effective concentration of the atoms at the reaction interface is expected to move further to the Zr-rich region until Zr_2Al_3 becomes the most likely phase to form. This process continues with subsequent phases richer in Zr being formed until the most zirconium-rich phase is formed. It has to be pointed out that unlike metal-silicon systems noncongruent phases are usually not skipped in metal-metal systems.[6,15] For thin Zr films on thick Al (Zr < Al) $ZrAl_3$ is again expected to be the first phase to form. When all the Zr is consumed the effective concentration of Al will tend to be greater than the composition of $ZrAl_3$ but as no further phases richer in Al exist no interaction is expected to take place and $ZrAl_3$ is the first and only phase to form. The effective heat of formation rule for phase formation sequence in metal-metal systems is thus formulated[7] as follows:

"*After first-phase formation in metal-metal binary systems, the next phase to form at the interface between the compound phase and remaining element is the next phase richer in the unreacted element, which has the most negative effective heat of formation.*"

Unfortunately experimental data for phase formation sequence in the Zr-Al system could not be found, but we find that the effective heat of formation rule generally predicts phase sequence successfully for nickel,[7,15,16] palladium,[17] platinum,[18] and gold[19] aluminides, except that skipping of certain phases is found for Pd, Pt, and Au. It would seem that phases are skipped that are difficult to

TABLE II. Heats of formation (ΔH^o) and effective heats of formation ($\Delta H'$) for various aluminides. The $\Delta H'$ values have been calculated at the concentration of the lowest temperature eutectic (liquidus) of the binary system. For systems without a lowest eutectic a relative effective concentration of 98 at. % Al and 2 at. % metal is arbitrarily chosen, as Al has in these cases the lowest melting temperature on the liquidus curve. The phases for which the $\Delta H'$ values are underlined are those that have been found to form first. References refer to work from which heats of formation (ΔH^o) were obtained. The number of atoms per unit cell are given in brackets behind each phase.

Phase	Composition	ΔH^o kJ (mol at.)$^{-1}$	Limiting element	$\Delta H'$ kJ (mol at.)$^{-1}$	Ref.
Lowest eutectic =	$Au_{0.780}Al_{0.220}$				
Au_4Al (20)	$Au_{0.800}Al_{0.200}$	-19	Au	-18.5	23
Au_5Al_2 (–)	$Au_{0.714}Al_{0.286}$	-26	Al	-20.0	23
Au_2Al (12)	$Au_{0.667}Al_{0.333}$	-30	Al	$\underline{-19.8}$	23
$AuAl$ (8)	$Au_{0.500}Al_{0.500}$	-37	Al	$\underline{-16.3}$	23
$AuAl_2$ (12)	$Au_{0.333}Al_{0.667}$	-31	Al	-10.2	23
Lowest eutectic =	$Co_{0.020}Al_{0.980}$ (1)				
$CoAl$ (2)	$Co_{0.500}Al_{0.500}$	-55	Co	-2.20	24
Co_2Al_5 (28)	$Co_{0.286}Al_{0.714}$	-42	Co	-2.94	24
$CoAl_3$ (4)	$Co_{0.250}Al_{0.750}$	-38	Co	-3.04	24
Co_4Al_{13} (100)	$Co_{0.235}Al_{0.765}$	-32	Co	-2.72	25
Co_2Al_9 (22)	$Co_{0.182}Al_{0.818}$	-30	Co	$\underline{-3.29}$	25
Lowest eutectic =	$Cr_{0.020}Al_{0.980}$ (1)				
Cr_2Al (6)	$Cr_{0.667}Al_{0.333}$	-11	Cr	-0.33	25
Cr_5Al_8 (26)	$Cr_{0.385}Al_{0.615}$	-15	Cr	-0.78	25
Cr_4Al_9 (52)	$Cr_{0.308}Al_{0.692}$	-16	Cr	-1.04	25
$CrAl_4$ (180)	$Cr_{0.200}Al_{0.800}$	-17	Cr	-1.70	25
Cr_2Al_{11} (48)	$Cr_{0.154}Al_{0.846}$	-15	Cr	-1.95	25
Cr_2Al_{13} (105)	$Cr_{0.125}Al_{0.875}$	-13	Cr	$\underline{-2.08}$	25
Lowest eutectic =	$Cu_{0.170}Al_{0.830}$				
Cu_5Al_3 (–)	$Cu_{0.625}Al_{0.375}$	-15	Cu	-4.08	23
$CuAl$ (20)	$Cu_{0.500}Al_{0.500}$	-15	Cu	-5.10	23
$CuAl_2$ (12)	$Cu_{0.333}Al_{0.667}$	-12	Cu	$\underline{-6.13}$	23
Lowest eutectic =	$Hf_{0.020}Al_{0.980}$ (1)				
Hf_2Al (12)	$Hf_{0.667}Al_{0.333}$	-41	Hf	-1.23	26
Hf_3Al_2 (20)	$Hf_{0.600}Al_{0.400}$	-44	Hf	-1.47	26
Hf_4Al_3 (7)	$Hf_{0.571}Al_{0.429}$	-46	Hf	-1.61	26
$HfAl$ (8)	$Hf_{0.500}Al_{0.500}$	-46	Hf	-1.84	26
Hf_2Al_3 (40)	$Hf_{0.400}Al_{0.600}$	-48	Hf	-2.40	26
$HfAl_2$ (12)	$Hf_{0.333}Al_{0.667}$	-48	Hf	-2.88	26
$HfAl_3$ (16)	$Hf_{0.250}Al_{0.750}$	-42	Hf	$\underline{-3.36}$	26
Lowest eutectic =	$Mo_{0.020}Al_{0.980}$ (1)				
Mo_3Al (8)	$Mo_{0.750}Al_{0.250}$	-50	Mo	-1.33	27
Mo_3Al_8 (22)	$Mo_{0.272}Al_{0.728}$	-49	Mo	-3.60	27
$MoAl_4$ (30)	$Mo_{0.200}Al_{0.800}$	-37	Mo	-3.70	27
Mo_4Al_{17} (–)	$Mo_{0.190}Al_{0.810}$	-36	Mo	-3.79	27
Mo_5Al_{22} (–)	$Mo_{0.185}Al_{0.815}$	-35	Mo	-3.78	27
$MoAl_5$ (12)	$Mo_{0.167}Al_{0.833}$	-32	Mo	-3.83	27
$MoAl_6$ (–)	$Mo_{0.143}Al_{0.857}$	-27	Mo	-3.78	27
$MoAl_{12}$ (26)	$Mo_{0.077}Al_{0.923}$	-15	Mo	$\underline{-3.90}$	27
Lowest eutectic =	$Nb_{0.020}Al_{0.980}$ (1)				
Nb_3Al (8)	$Nb_{0.750}Al_{0.250}$	-19	Nb	-0.51	28
Nb_2Al (30)	$Nb_{0.667}Al_{0.333}$	-25	Nb	-0.75	28
$NbAl_3$ (8)	$Nb_{0.250}Al_{0.750}$	-33	Nb	$\underline{-2.64}$	28
Lowest eutectic =	$Ni_{0.035}Al_{0.965}$				
Ni_3Al (4)	$Ni_{0.750}Al_{0.250}$	-41	Ni	-1.91	25
$NiAl$ (2)	$Ni_{0.500}Al_{0.500}$	-59	Ni	-4.13	25
Ni_2Al_3 (5)	$Ni_{0.400}Al_{0.600}$	-57	Ni	-4.99	25
$NiAl_3$ (16)	$Ni_{0.250}Al_{0.750}$	-38	Ni	$\underline{-5.32}$	25
Lowest eutectic =	$Pd_{0.080}Al_{0.920}$				
Pd_2Al (12)	$Pd_{0.667}Al_{0.333}$	-85	Pd	-10.19	25

TABLE II. (*Continued.*)

Phase	Composition	ΔH kJ (mol at.)$^{-1}$	Limiting element	$\Delta H'$ kJ (mol at.)$^{-1}$	Ref.
PdAl (26)	$Pd_{0.500}Al_{0.500}$	− 92	Pd	− 14.72	25
Pd_2Al_3 (5)	$Pd_{0.400}Al_{0.600}$	− 83	Pd	− 16.60	25
$PdAl_3$ (−)	$Pd_{0.250}Al_{0.750}$	− 52	Pd	− 16.64	25
$PdAl_4$ (90)	$Pd_{0.200}Al_{0.800}$	− 40	Pd	− 16.00	29
Lowest eutectic =	$Pt_{0.020}Al_{0.980}$ (1)				
Pt_3Al (16)	$Pt_{0.750}Al_{0.250}$	− 70	Pt	− 1.87	30
Pt_2Al (24)	$Pt_{0.667}Al_{0.333}$	− 88	Pt	− 2.64	30
Pt_5Al_3 (16)	$Pt_{0.625}Al_{0.375}$	− 88	Pt	− 2.82	30
PtAl (8)	$Pt_{0.500}Al_{0.500}$	− 100	Pt	− 4.00	30
Pt_2Al_3 (5)	$Pt_{0.400}Al_{0.600}$	− 95	Pt	− 4.75	30
$PtAl_2$ (12)	$Pt_{0.333}Al_{0.667}$	− 84	Pt	− 5.05	30
Pt_8Al_{21} (116)	$Pt_{0.276}Al_{0.724}$	− 72	Pt	− 5.14	30
$PtAl_4$ (90)^a	$Pt_{0.200}Al_{0.800}$	− 57	Pt	− 5.70	30
Pt_5Al_{21} (416)	$Pt_{0.192}Al_{0.808}$	− 57	Pt	− 5.94	30
Lowest eutectic =	$Ta_{0.020}Al_{0.980}$ (1)				
Ta_2Al (30)	$Ta_{0.667}Al_{0.333}$	− 37	Ta	− 1.11	23
$TaAl_3$ (8)	$Ta_{0.250}Al_{0.750}$	− 30	Ta	− 2.40	23
Lowest eutectic =	$Ti_{0.020}Al_{0.980}$ (1)				
Ti_3Al (8)	$Ti_{0.750}Al_{0.250}$	− 25	Ti	− 0.67	25
Ti_2Al (−)	$Ti_{0.667}Al_{0.333}$	− 50	Ti	− 1.49	23
TiAl (4)	$Ti_{0.500}Al_{0.500}$	− 38	Ti	− 1.52	25
$TiAl_3$ (8)	$Ti_{0.250}Al_{0.750}$	− 37	Ti	− 2.96	25
Lowest eutectic =	$V_{0.020}Al_{0.980}$ (1)				
V_5Al_8 (52)	$V_{0.385}Al_{0.615}$	− 35	V	− 1.82	23
VAl_3 (8)	$V_{0.250}Al_{0.750}$	− 24	V	− 1.92	23
V_4Al_{23} (54)	$V_{0.143}Al_{0.857}$	− 14	V	− 1.95	23
VAl_7 (104)	$V_{0.125}Al_{0.875}$	− 12	V	− 1.92	23
VAl_{10} (176)	$V_{0.091}Al_{0.909}$	− 8	V	− 1.98	23
Lowest eutectic =	$W_{0.020}Al_{0.980}$ (1)				
WAl_4 (30)	$W_{0.200}Al_{0.800}$	− 10.4	W	− 1.04	23
WAl_5 (12)	$W_{0.167}Al_{0.833}$	− 9.0	W	− 1.07	23
WAl_{12} (26)	$W_{0.077}Al_{0.923}$	− 4.0	W	− 1.03	23
Lowest eutectic =	$Zr_{0.020}Al_{0.980}$ (1)				
Zr_5Al_3 (16)	$Zr_{0.625}Al_{0.375}$	− 39	Zr	− 1.25	31
Zr_3Al_2 (20)	$Zr_{0.600}Al_{0.400}$	− 41	Zr	− 1.37	31
Zr_4Al_3 (7)	$Zr_{0.571}Al_{0.429}$	− 43	Zr	− 1.51	25
ZrAl (8)	$Zr_{0.500}Al_{0.500}$	− 45	Zr	− 1.80	31
Zr_2Al_3 (40)	$Zr_{0.400}Al_{0.600}$	− 47	Zr	− 2.35	31
$ZrAl_2$ (12)	$Zr_{0.333}Al_{0.667}$	− 46	Zr	− 2.76	31
$ZrAl_3$ (16)	$Zr_{0.250}Al_{0.750}$	− 41	Zr	− 3.28	31

^{a}Metastable phase.

nucleate which is usually indicated by a large number of atoms per unit cell or by noncongruency.

C. Au-Al system

Due to its importance in semiconductor device metallurgy, the Au-Al system has been the subject of considerable attention. The Au-Al phase diagram shows five stoichiometric compounds namely Au_4Al, Au_5Al_2, Au_2Al, AuAl, and $AuAl_2$ (see Fig. 2). Thin-film studies using Rutherford backscattering spectrometry and x-ray diffraction have been used to determine growth kinetics and phase formation sequence[19–22] in this system. There is much uncertainty regarding first phase formation as certain measurements show that Au_5Al_2 and Au_2Al start to grow simultaneously[20] while others have found only Au_5Al_2 to be the first phase to form.[19,21,22]

Using the effective heat of formation concept to predict first phase formation we see that there is from a thermodynamic point of view hardly any difference between Au_5Al_2 and Au_2Al formation (see effective heat of formation diagram in Fig. 2). At the composition of the lowest eutectic (78 at. % Au, 22 at. % Al) the $\Delta H'$ value for Au_5Al_2 is − 20.0 kJ(mol at.)$^{-1}$ and − 19.8
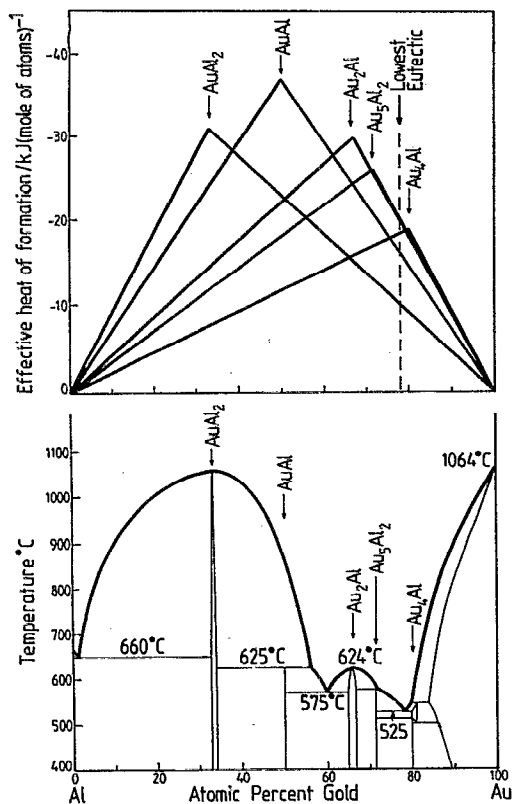
FIG. 2. Effective heat of formation diagram and phase diagram for the Al-Au system. This system is very interesting as it is one of the few cases where the lowest eutectic (liquidus) is not Al rich.

kJ(mol at.)$^{-1}$ for Au$_2$Al (see Table II). This difference is negligibly small and differences in experimental conditions could thus favor formation of one or the other. This is confirmed by experimental results.[19-22] The formation of both Au$_5$Al$_2$ and Au$_2$Al as found by Campisano et al.[20] is probably due to small variations in the effective concentrations laterally along the growth interface due to for instance impurities. If conditions are exactly identical along the entire growth interface, formation of only one phase would be expected.

The Bené rule[6] states that the first phase nucleated in metal-metal thin-film reactions is the phase immediately adjacent to the low-temperature eutectic in the binary phase diagram. If we look at the Au-Al binary phase diagram (bottom, Fig. 2) we see that the predicted first phase according to this rule is Au$_4$Al. As discussed above, the effective heat of formation rule correctly predicts either Au$_5$Al$_2$ or Au$_2$Al (top, Fig. 2).

D. Pt-Al system

The Pt-Al system is very complicated with many equilibrium phases.[11] In Table III some crystallographic and thermodynamic data are given for these phases with the high-temperature phases of Pt$_3$Al, Pt$_2$Al, and PtAl being omitted as thin-film interaction studies are usually carried out at temperatures below 800 °C. From Table III and Fig. 3 it can be seen that the phase Pt$_5$Al$_{21}$ has the most negative effective heat of formation, namely −5.94

TABLE III. Crystallographic and thermodynamic data for equilibrium Pt-aluminide phases. The effective heats of formation ($\Delta H'$) have been calculated at a concentration of 2 at. % Pt and 98 at. % Al.

Phase	Crystal system	Lattice constants (nm)	Atoms per unit cell	ΔH^o kJ (mol at.)$^{-1}$	$\Delta H'$ kJ (mol at.)$^{-1}$
Pt$_3$Al[a,b]	tetrag.	0.5459 0.7806	16	−70	−1.87
Pt$_2$Al[a]	orthor.	1.6306 0.3919 0.5433	24	−88	−2.64
Pt$_5$Al$_3$	orthor.	0.541 1.070 0.395	16	−88	−2.82
PtAl[a,b]	cubic	0.4866	8	−100	−4.00
Pt$_2$Al$_3$[b]	hexag.	0.4209 1.035	5	−95	−4.75
PtAl$_2$[b]	cubic	0.5910	12	−84	−5.05
Pt$_8$Al$_{21}$	tetrag.	1.297 1.065	116	−71	−5.14
Pt$_5$Al$_{21}$	cubic	···	416	−57	−5.94

[a]Also has a high-temperature phase.
[b]Phases definitely observed in thin-film studies.

kJ(mol at.)$^{-1}$. Its formation would thus be expected to lead to the largest change in free energy. Most thin-film studies do, however, show that Pt$_2$Al$_3$ is the first phase to form.[18,32,33] This is very interesting since, in most cases, the
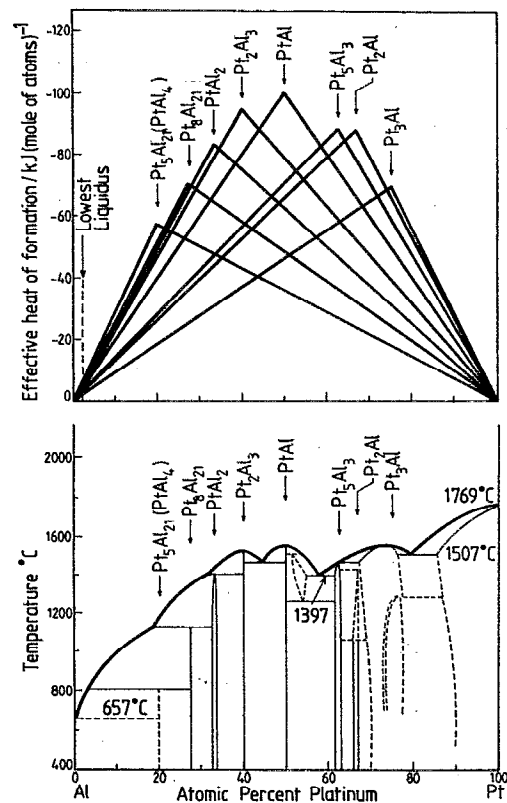

FIG. 3. The effective heat of formation and phase diagrams for the Pt-Al system. The compound PtAl$_4$ is not an equilibrium phase and has only been observed after heating of thin-film structures.

3641   J. Appl. Phys., Vol. 70, No. 7, 1 October 1991

Pretorius et al.   3641

formation of the most Al-rich phase (Pt_5Al_{21} in this case) is usually the norm for Al transition metal reaction, as can be seen from the excellent review article and thesis on aluminides by Colgan.[34] Table III does, however, show that the Pt_5Al_{21} phase has 416 atoms per unit cell, it would thus have great difficulty in nucleating, especially in a non-equilibrium situation, such as in thin-film systems, where growth has to take place at a moving interface. The Pt_8Al_{21} phase would also be difficult to nucleate as it has 116 atoms per unit (see Table III). Taking nucleation into consideration, the effective heat of formation rule would thus predict first phase formation of either $PtAl_2$ (12 atoms per unit cell) or Pt_2Al_3 (5 atoms per unit cell). Their $\Delta H'$ values are -5.05 and -4.75 kJ(mol at.)$^{-1}$, respectively, and if it is kept in mind that thermodynamic quantities are seldom known with accuracies better than 10% it is clear that there is not much to choose between $PtAl_2$ and Pt_2Al_3 formation from a thermodynamic point of view. It is nevertheless interesting that Pt_2Al_3 is usually found to form first instead of $PtAl_2$.[18,32,33]

It has to be emphasized that the effective heat of formation rule predicts that if it were not for nucleation barriers, formation of the most Al-rich phase Pt_5Al_{21} (see Table III) would lead to the largest change in free energy. In this context it is interesting that Howard et al.[13] found that $PtAl_4$, metastable phase with composition very close to that of Pt_5Al_{21}, is the first phase to form and that it grows parabolically with time between 250 °C and 350 °C. Colgan,[18] although finding Pt_2Al_3 first phase formation in thin-film systems, also observes subsequent $PtAl_4$ formation at higher temperatures when he has an overall Al-rich stoichiometry. The $PtAl_4$ phase, which is simpler than the Pt_5Al_{21} phase (90 vs 416 atoms per unit cell) did not form until 450 °C. It appears that higher temperatures are needed to nucleate $PtAl_4$ than Pt_2Al_3 which starts to form at 225 °C.[18] This is understandable as higher temperatures lead to greater mobility and easier nucleation of phases, especially those with many atoms per unit cell. Because $PtAl_4$ is a metastable phase it is difficult to determine its heat of formation. However, since $PtAl_4$ has a composition very close to that of Pt_5Al_{21} it can be expected, according to Miedema (see Ref. 23), that $PtAl_4$ should have a heat of formation very close to that of Pt_5Al_{21}, namely -57 kJ(mol at.)$^{-1}$ (see Table III). It is clear that the effective heat of formation rule is very successful in interpreting experimental observations in Pt-Al thin-film systems.[13,18,32,33,35]

As far as phase sequence is concerned, the effective heat of formation rule predicts that after first phase Pt_2Al_3 formation, this phase will continue growing until either all the Al or all the Pt is consumed. For thin Al on thick Pt (Pt > Al), all the Al is consumed and the effective concentration of Al is expected to decrease, the relative concentrations of the reactants moving to the right of the effective heat of formation diagram (see Fig. 3) to a concentration region where PtAl formation leads to the biggest change in free energy. After transformation of all the Pt_2Al_3 to PtAl the effective concentration of the atoms moves further to the Pt-rich region and Pt_5Al_3 formation is

most likely to form at the Pt/PtAl interface, followed by Pt_2Al, and finally Pt_3Al, as this is the most Pt-rich phase. Experimental measurement shows that this is indeed the sequence of phase formation in the Pt-Al system, although there is some uncertainty as to the formation of Pt_5Al_3 and Pt_2Al.[18] For structures with thin Pt in contact with thick Al (Al > Pt), Pt_2Al_3 is again predicted to form first until all the Pt is used up, followed by formation of $PtAl_2$ and $PtAl_4$. The phases Pt_8Al_{21} and Pt_5Al_{21} are not expected to form because of their difficulty to nucleate, as discussed above. Rutherford backscattering spectrometry and x-ray diffraction measurements do show that Pt_2Al_3 forms first, but that $PtAl_2$ is then skipped, with $PtAl_4$ formation taking place as the final phase.[18] It is, however, interesting to note that $PtAl_2$, Pt_8Al_{21}, and Pt_5Al_{21} are also all noncongruent phases and that in metal-silicon systems it is generally found that noncongruent phases are skipped.[1,10]

E. Other binary metal-Al systems

In Table II the heats of formation (ΔH°) and effective heats of formation ($\Delta H'$) are given for metal-Al binary systems, for which heats of formation and experimental data regarding first phase formation could be found. It should be pointed out that the absolute values of $\Delta H'$ are of no importance and that the effective heats of formation should only be compared for a particular binary system. The phases for which the $\Delta H'$ values are underlined are those that have been found experimentally to have formed first. In Table IV these results are summarized. The predicted phases are those with the most negative effective heat of formation. More than one phase is predicted in those cases where other phases have $\Delta H'$ values within 5% of the most negative effective heat of formation. Phases with a large number of atoms per unit cell (such as Pt_8Al_{21} and Pt_5Al_{21}) are not expected to be the first phase to form, even though they may have the most negative $\Delta H'$ values. This is because they are difficult to nucleate. In the case of the Pt-Al system, therefore, $PtAl_2$ is taken as the phase with the most negative effective heat of formation.

From Table IV it is clear that in every case, the effective heat of formation rule correctly predicts the observed first phase formation. It is also interesting to note that in the case of the Au-Al system, where both Au_5Al_2 and Au_2Al are predicted and where the difference between their $\Delta H'$ values are very small, both phase have been found to form first or simultaneously.[19-22] The same applies to the Pd system. The Mo-Al system is also very interesting as there is a very small difference from a thermodynamic point of view, between five different phases ranging from Mo_4Al_{17} to $MoAl_{12}$. Although $MoAl_{12}$ has been found to be the first phase to form,[40,50] the system is expected to be very sensitive to factors such as impurities which can affect the effective concentrations of the reactants and thus swing the first phase formation to one of the other phases.

From the second row of Table IV it can be seen that with the exception of the Au-Al system all the metal-Al binary systems have a lowest temperature eutectic (or liquidus) which is overwhelmingly Al rich. The effective

TABLE IV. Comparison of observed first phase formation and predicted first phase in metal-aluminum systems using the effective heat of formation ($\Delta H'$) rule. The effective heat of formation is calculated at the concentration of the lowest temperature eutectic (liquidus) of the binary phase diagram. The predicted phases are those with effective heats of formation ($\Delta H'$) within 5% of the most negative $\Delta H'$ (see Table II).

System	Lowest eutectic (at. % Al)	Predicted phases	Atoms per unit cell	$\Delta H'$ kJ(mol at.)$^{-1}$	Observed phases	References
Au	22	Au_5Al_2	...	− 20.0	Au_5Al_2	19–22
		Au_2Al	12	− 19.8	Au_2Al	20
Co	98(1)	Co_2Al_9	22	− 3.29	Co_2Al_9	13,35,40
Cr	98(1)	Cr_2Al_{11}	48	− 1.95		
		Cr_2Al_{13}[a]	105	− 2.08	Cr_2Al_{13}	13,36,37,40
Cu	83	$CuAl_2$	12	− 6.13	$CuAl_2$	6
Hf	98(1)	$HfAl_3$	16	− 3.36	$HfAl_3$	13,38,39
Mo	98(1)	Mo_4Al_{17}	...	− 3.79		
		Mo_5Al_{22}	...	− 3.78		
		$MoAl_5$	12	− 3.83		
		$MoAl_6$	...	− 3.78		
		$MoAl_{12}$	26	− 3.90	$MoAl_{12}$	40,50
Nb	98(1)	$NbAl_3$	8	− 2.64	$NbAl_3$	40,51,52
Ni	96.5	$NiAl_3$	16	− 5.32	$NiAl_3$	16,35,41,42
Pd	92.0	Pd_2Al_3	5	− 16.6	Pd_2Al_3	17,42
		$PdAl_3$	...	− 16.6	$PdAl_3$	13
		$PdAl_4$	90	− 16.0	$PdAl_4$	33,35
Pt	98(1)	Pt_2Al_3	5	− 4.75	Pt_2Al_3	18,32,33,35,53,54
		$PtAl_2$	12	− 5.05		
		Pt_8Al_{21}	116	− 5.14		
		$PtAl_4$[b]	90	− 5.70	$PtAl_4$	13
		Pt_5Al_{21}	416	− 5.94		
Ta	98(1)	$TaAl_3$	8	− 2.40	$TaAl_3$	13,35,40,43
Ti	98(1)	$TiAl_3$	8	− 2.96	$TiAl_3$	13,14,35,38,40,44,46
V	98(1)	VAl_3	8	− 1.92	VAl_3	44,47,48
		V_4Al_{23}	54	− 1.95		
		VAl_7	104	− 1.92		
		VAl_{10}	176	− 1.98	VAl_{10}	47,48
W	98(1)	WAl_4	30	− 1.04		
		WAl_5	12	− 1.07		
		WAl_{12}	26	− 1.03	WAl_{12}	40,45,49
Zr	98(1)	$ZrAl_3$	16	− 3.28	$ZrAl_3$	13,14,39

[a]This phase is identical to $CrAl_7$ which is the phase referred to in older Refs. (34 and 40).
[b]Metastable phase.

heat of formation rule for first phase formation thus explains in a quantitative way why the Al-rich phase is usually always favored.

F. Decomposition

Colgan[34] has measured formation and decomposition of several aluminide phases in contact with each other or in contact with their component metals. In Table V his experimental results are compared with effective heat of formation first phase predictions. To illustrate the use of the

effective heat of formation rule in such structures we will discuss the Ni-Al system.

The effective heat of formation diagram for the Ni-Al binary system is given in Fig. 4, with the composition of the different structures that have been investigated represented schematically above. During heating of the Al/Ni$_3$Al structure, mixing at the interface is again, as was the case for Ni/Al samples, expected to take place (see Fig. 4) at the concentration of the lowest eutectic (3.5 at. % Ni, 96.5 at. % Al). At this effective concentration

TABLE V. Decomposition of aluminide phases in contact with each other or in contact with their component metals. The predicted phase was obtained using the effective heat of formation rule in conjunction with the concentration of the lowest melting point eutectic of the binary system.

System	Sample	Predicted phases	Observed phase[a]
Ni	Al/Ni$_3$Al	NiAl$_3$	NiAl$_3$
	NiAl$_3$/Ni	Ni$_2$Al$_3$	Ni$_2$Al$_3$
	NiAl$_3$/Ni$_3$Al	Ni$_2$Al$_3$	Ni$_2$Al$_3$
	Al/NiAl/Ni	NiAl$_3$	NiAl$_3$
Pd	Al/Pd$_2$Al	Pd$_2$Al$_3$, PdAl$_3$, PdAl$_4$	Pd$_2$Al$_3$
	Al/PdAl/Pd	Pd$_2$Al$_3$, PdAl$_3$, PdAl$_4$	Pd$_2$Al$_3$
	Pd$_2$Al$_3$/Pd	PdAl	PdAl
Pt	Al/Pt$_2$Al	PtAl$_2$, Pt$_2$Al$_3$	Pt$_2$Al$_3$
	PtAl$_2$/Pt	PtAl$_2$, Pt$_2$Al$_3$	Pt$_2$Al$_3$
	Al/Pt$_5$Al$_{21}$/Pt	PtAl$_2$, Pt$_2$Al$_3$	Pt$_2$Al$_3$
	Pt$_2$Al$_3$/Pt	PtAl	PtAl
Ti	Al/TiAl/Ti	TiAl$_3$	TiAl$_3$
V	Al/VAl$_{10}$/V	VAl$_3$	VAl$_3$

[a]References: Ni(16), Pd(17), Pt(18), Ti and V from E. G. Colgan, Ph.D. thesis, Cornell University, 1987.

NiAl$_3$ is expected to be the first phase to form as was the case for the Ni/Al system. For the NiAl$_3$/Ni structure the effective concentration at the reaction interface is again controlled by the lowest eutectic, and will be on the Al-rich side within the NiAl$_3$ to Ni concentration range. The ef-
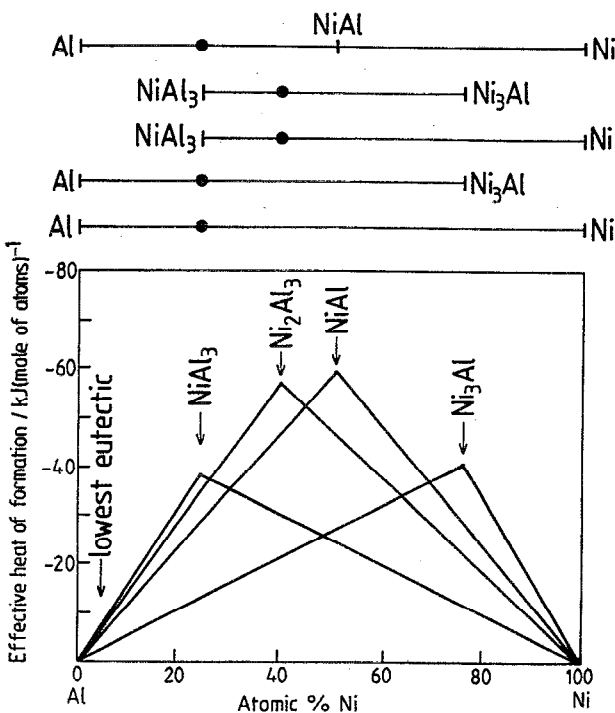

FIG. 4. The Ni-Al effective heat of formation diagram. Various structures for which phase formation and decomposition have been studied are shown at the top. The first phase formed in each case is indicated by the dot on the concentration axis.

fective heat of formation diagram in Fig. 4, therefore, predicts that Ni$_2$Al$_3$ should form. The situation is similar to that for thin Al on thick Ni, after all the aluminum has been consumed during first phase NiAl$_3$ formation. The effective heat of formation rule for phase sequence states that the phase formed will be the next phase richer in the unreacted element (Ni), which has the most negative effective heat of formation. For the NiAl$_3$/Ni$_3$Al structure the effective concentration is again controlled by the lowest eutectic, which is on the Al side of the phase diagram. Ni$_2$Al$_3$ is again expected to form as it is the most Al-rich phase between the compositions of the two initial phases (see Fig. 4). When an Al/NiAl/Ni structure is heated, the lowest eutectic of the Al/Ni system being at 96.5 at. % Al will again cause an Al-rich effective concentration at the Al/NiAl interface leading to NiAl$_3$ formation. At the NiAl/Ni interface the only phase that can form is Ni$_3$Al; however, its reaction rate is expected to be much slower, as the interface composition is further away from the lowest eutectic and less mobility of the atoms can thus be expected. In summary, whatever the configuration of a specific sample, mixing at the interface(s) will always be controlled by the lowest temperature eutectic of the system and the effective concentrations will be expected to be as close as possible to that of the lowest eutectic within the concentration range of the two interacting phases. This will be so even if the eutectic composition does not lie between the compositions of the interacting phases. Phases will react with each other to form the most Al-rich phase (with the exception of the Au-Al system where the lowest eutectic is on the Au-rich side of the phase diagram) with a composition lying between that of the interacting phases. Reaction to form a phase outside this composition range can only lead to an increase in free energy, as it leads to less bond formation.

From Table V it can be seen that in every case the effective heat of formation rule ($\Delta H'$) correctly predicts the initial phase formation. This is in contrast to the efforts by Colgan[16–18,34] who was unsuccessful when trying to use equilibrium thermodynamics and without taking concentration into account to predict phase formation and decomposition in these structures.

IV. SUMMARY AND CONCLUSION

The effective heat of formation concept makes it possible to calculate heats of formation as a function of the relative concentrations of the reactant-atomic species. As phase formation during solid state interaction is a dynamic nonequilibrium process, an effective concentration at the growth interface is defined that differs from the true physical concentrations at the growth interface. This is similar to the effective concentration concept in solution chemistry where the effective concentration is linked to the true concentration by an activity coefficient. Although the effective concentrations could be influenced by many factors such as impurities, diffusing species, diffusivity, kinetics, temperature, etc., the overriding factor apparently affecting concentrations at a growth interface is the lowest temperature eutectic (or liquidus when the lowest eutectic temperature

is not the lowest on the liquidus curve). We therefore choose the concentration at the lowest eutectic (liquidus) as the effective concentration at the growth interface, as mixing and interdiffusion is most likely to occur at such a concentration during heating. This criterion is also used by Walser and Bené in their rules for prediction of phase formation.[1,6] Because the entropy change during solid state interaction is usually very small, the heat of formation is a good measure of the free energy change for the system. Although the effective heat of formation rule for first phase formation may predict that formation of a particular phase would lead to the largest free energy change, the phase may not be able to form due to a nucleation barrier. This is for instance the case for the Pt-Al binary system where the effective heat of formation rule predicts that Pt_5Al_{21} and Pt_8Al_{21} have the most negative effective heats of formation (see Table III). These phases do, however, have 416 and 116 atoms per unit cell, respectively, and would thus have great difficulty to nucleate at a moving interface. If such phases are excluded, the effective heat of formation rule predicts first phase formation correctly for all 15 metal-aluminum binary systems for which experimental data could be obtained (see Table IV). In nearly all the cases the most Al-rich phase is formed first (see Table II), due to the fact that the lowest eutectic (liquidus) is always at a composition that is very aluminum-rich (with the exception of Au), namely between 83 and 100 at. % Al. Exceptions are V, Pd, and Pt as their most Al-rich phases are difficult to nucleate because of the large number of atoms per unit cell. The Au-Al system is very interesting as it is the only one that has a lowest eutectic (liquidus) that is not Al rich (22 at. % Al, 78 at. % Au). The effective heat of formation rule predicts that there is from a thermodynamic point of view little to choose between the formation of Au_5Al_2 and Au_2Al and this is supported by experimental results where the formation of Au_5Al_2 (Refs. 19, 21, and 22) and Au_2Al (Ref. 20) has been found. The same applies to the Pd-Al system where Pd_2Al_3, $PdAl_3$, and $PdAl_4$ are predicted and have been found to form (see Table IV) as first phases.[13,17,26,33]

Unlike the Walser and Bené rules,[1,6] which are rather empirical, the effective heat of formation rule makes direct use of thermodynamic data. It in effect gives a quantitative reason for the relatively large margin of success of the Walser and Bené rules.[1,6] The more accurate predictions achievable with the effective heat of formation rule is clearly illustrated by the Au-Al system.

The phase formation sequence in binary metal-aluminum thin-film systems depends on the overall composition of the structure. For thin Al films on thick metal ($M > Al$) the first phase to form is the one predicted by the effective heat of formation rule, which is usually Al rich. After all the Al is used up during first phase formation the effective concentration of Al at the growth interface decreases and the next phase to form is the next phase richer in the unreacted metal, which has the most negative effective heat of formation. This continues until all of the first phase is used up during formation of the second phase. This process continues with subsequent phases richer in the unreacted

metal being formed until the most metal rich (lowest Al content) is formed. For thin metal films on thick Al ($M < Al$), the same first phase formation takes place but now Al is the remaining element and the effective concentration tends to be more Al rich leading to formation of the adjacent phase which is more Al rich, the process ending when the most Al-rich phase has formed. However, since the most Al-rich phase is usually the first phase to form no subsequent phase formation takes place. Phase skipping does not take place in cases such as Ni, but for Pd, Pt, and Au, skipping is found to occur for phases that are difficult to nucleate, which is usually indicated by a large number of atoms per unit cell or by noncongruency.

The effective heat of formation concept has also been found to be very successful in predicting phase formation or stability of aluminide phases in contact with each other or with their component metals. It is found that whatever the configuration of a specific sample, phase formation is controlled by the lowest eutectic (liquidus) and the effective concentrations at the growth interface is expected to be as close as possible to that of the lowest temperature eutectic (liquidus) within the concentration range of the two interacting phases. Phases will thus react with each other to form a phase with a composition between that of the interacting phases and closest to that of the lowest eutectic (liquidus) composition.

To summarize, the effective heat of formation concept enables the calculation of heats of formation as a function of concentration. By using the composition of the lowest eutectic (liquidus) of the binary system as a measure of the relative effective concentrations of the reactants, rules can be formulated to predict first phase formation and phase formation sequence. The effective heat of formation rule used in conjunction with ease of nucleation (complex phases with large numbers of atoms per unit cell have problems nucleating, especially at a moving interface) successfully predicts first phase formation, phase formation sequence, and decomposition of phases for all 15 metal-aluminum binary systems for which experimental data could be found.

ACKNOWLEDGMENTS

[1] R. M. Walser and R. W. Bené, Appl. Phys. Lett. 28, 624 (1976).
[2] B. Y. Tsaur, S. S. Lau, J. W. Mayer, and M.-A. Nicolet, Appl. Phys. Lett. 38, 922 (1981).
[3] M. Ronay, Appl. Phys. Lett. 42, 577 (1983).
[4] R. Pretorius, Mater. Res. Soc. Proc. 25, 15 (1984).
[5] R. Pretorius, Vacuum 41, 1038 (1990).
[6] R. W. Bené, Appl. Phys. Lett. 41, 529 (1982).

[7] R. Pretorius, R. de Reus, A. M. Vredenberg, and F. W. Saris, Mater. Lett. **9**, 494 (1990).

[8] W. Xia, C. A. Hewett, M. Fernandes, S. S. Lau, and D. B. Poker, J. Appl. Phys. **65**, 2300 (1989).

[9] O. Kubaschewski and C. B. Alcock, *Metallurgical Thermochemistry*, 5th ed. (Pergamon, Oxford, 1979), p. 268.

[10] M.-A. Nicolet and S. S. Lau, in *VLSI Electronics: Microstructure Science*, edited by N. Einspruch (Academic, New York, 1983), Vol. 6, p. 329.

[11] T. B. Massalski, *Binary Alloy Phase Diagrams* (American Society for Metals Park, Ohio, 1986).

[12] A. M. Brown and M. F. Ashby, Acta Metall. **24**, 1088 (1980).

[13] J. K. Howard, R. F. Lever, P. J. Smith, and P. S. Ho, J. Vac. Sci. Technol. **13**, 68 (1976).

[14] M. Wittmer, F. LeGoues, and H.-C. W. Huang, J. Electrochem. Soc. **132**, 1450 (1985).

[15] E. G. Colgan and J. W. Mayer, Mater. Res. Soc. Symp. Proc. **54**, 121 (1986).

[16] E. G. Colgan, M. Nastasi, and J. W. Mayer, J. Appl. Phys. **58**, 4125 (1985).

[17] E. G. Colgan, J. Appl. Phys. **62**, 2269 (1987).

[18] E. G. Colgan, J. Appl. Phys. **62**, 1224 (1987).

[19] G. Majni, C. Nobili, G. Ottaviani, M. Costato, and E. Galli, J. Appl. Phys. **52**, 4047 (1981).

[20] S. U. Campisano, G. Foti, E. Rimini, S. S. Lau, and J. W. Mayer, Philos. Mag. **31**, 903 (1975).

[21] G. Majni, G. Ottaviani, and E. Galli, J. Cryst. Growth **47**, 583 (1979).

[22] J. M. van den Berg and R. A. Hamm, J. Vac. Sci. Technol. **19**, 156 (1981).

[23] F. R. de Boer, R. Boom, W. C. M. Mattens, A. R. Miedema, and A. K. Niessen, *Cohesion in Metals*, edited by F. R. de Boer and D. G. Pettifor (North Holland, Amsterdam 1988), Vol. 1 of the Series on Cohesion and Structure.

[24] I. Barin, O. Knacke, and O. Kubaschewski, *Thermochemical Properties of Inorganic Substances*, Supplement (Springer, Berlin, 1977).

[25] R. Hultgren, P. D. Desai, D. T. Hawkins, M. Gleiser, and K. K. Kelley, *Selected Values of the Thermodynamic Properties of Binary Alloys* (American Society for Metals, Metals Park, OH, 1973).

[26] P. J. Spencer, At. Energy Rev. Spec. Issue **8**, 9 (1981).

[27] L. Brewer and R. H. Lamoreaux, At. Energy Rev. Spec. Issue **7**, 11 (1980).

[28] I. Shilo, H. F. Franzen, and R. A. Schiffman, J. Electrochem. Soc. **129**, 1608 (1982).

[29] R. Ferro and R. Capelli, Atti Accad. Naz. Lincei Cl. Sci. Fis. Mat. Nat. Rend. **34**, 659 (1963).

[30] R. Ferro, A. Capelli, A. Borsese, and G. Centineo, Att. Accad. Naz. Lincei Cl. Sci. Fis. Mat. Nat. Rend. **45**, 54 (1968).

[31] R. J. Kematick and H. F. Franzen, J. Solid State Chem. **54**, 226 (1984).

[32] S. P. Murarka, I. A. Blech, and H. J. Levinstein, J. Appl. Phys. **47**, 5175 (1976).

[33] M. Nastasi, L. S. Hung, and J. W. Mayer, Appl. Phys. Lett. **43**, 831 (1983).

[34] E. G. Colgan, Mater. Sci. Rep. **5**, 1 (1990); E. G. Colgan, Ph.D. thesis, Cornell University, Ithaca, NY, 1987.

[35] J. K. Howard, J. F. White, and P. S. Ho, J. Appl. Phys. **49**, 4083 (1978).

[36] J. K. Howard, W. K. Chu, and R. F. Lever, *Ion Beam Surface Layer Analysis*, edited by O. Meyer, G. Linker, and F. Kapeller (Plenum, New York, 1976), Vol. 1, p. 125.

[37] M. B. Chamberlain, J. Vac. Sci. Technol. **16**, 339 (1979).

[38] H. C. W. Huang and M. Wittmer, Mater. Res. Soc. Proc. **25**, 157 (1984).

[39] R. F. Lever, J. K. Howard, W. K. Chu, and P. J. Smith, J. Vac. Sci. Technol. **14**, 158 (1977).

[40] E. G. Colgan and J. W. Mayer, J. Mater. Res. **4**, 815 (1989).

[41] J. E. E. Baglin and F. M. d'Heurle, *Ion Beam Surface Layer Analysis*, edited by O. Meyer, G. Linker and F. Kappeler (Plenum, New York, 1976), Vol. 1, p. 385.

[42] U. Koster, P. S. Ho, and M. Ron, Thin Solid Films **67**, 35 (1980).

[43] J. W. Liaw, Y.-C. Liu, J. S. Maa, W. S. Hsu, W. J. Shen, and S. K. H. Siung, Tsai Liao K'o Hsueh **12**, 36 (1980).

[44] K. Nakamura, S. S. Lau, M.-A. Nicolet, and J. W. Mayer, Appl. Phys. Lett. **28**, 277 (1976).

[45] I. Krafesik, J. Gyulai, C. J. Palmström, and J. W. Mayer, Appl. Phys. Lett. **43**, 1015 (1983).

[46] J. Tardy and K. N. Tu, Phys. Rev. B **32**, 2070 (1985).

[47] M. Eizenberg, R. D. Thompson, and K. N. Tu, J. Appl. Phys. **53**, 6891 (1982).

[48] T. G. Finstad, G. Salomonsen, N. Norman, and J. S. Johannessen, Thin Solid Films **114**, 271 (1984).

[49] G. J. van Gurp, J. L. C. Daams, A. van Oostrom, L. J. M. Augustus, and Y. Tamminga, J. Appl. Phys. **50**, 6915 (1979).

[50] M. Kitada and N. Shimizu, J. Mater. Sci. **19**, 1339 (1984).

[51] R. K. Ball and A. G. Todd, Thin Solid Films **149**, 269 (1987).

[52] K. R. Coffey, L. A. Clevenger, K. Barmak, D. A. Rudman, and C. V. Thompson, Appl. Phys. Lett. **55**, 852 (1989).

[53] E. Ma and M.-A. Nicolet, Phys. Status Solidi A **110**, 509 (1988).

[54] X. A. Zhao, E. Ma, H. Y. Yang, and M. A. Nicolet, Thin Solid Films **153**, 379 (1987).

3646   J. Appl. Phys., Vol. 70, No. 7, 1 October 1991

Pretorius *et al.*   3646